Engineering an electron-asymmetric Fe_2O_3-CeO_2 nanowire array heterostructure for efficient nitrogen reduction reaction under ambient condition

Jiujiang Xian,[a] Yushu Gou,[b] Yuanming Mu,[a] Shilin Zhang,[a*] Yuyao Ji[a*]

[a]College of Chemistry and Materials Science, Sichuan Normal University, Chengdu 610068, China. E-mail: slzhang@sicnu.edu.cn, yyji@sicnu.edu.cn

[b]School of Healthcare Technology, Chengdu Neusoft University, 611844, Sichuan, China

Content:

Experimental section

Materials： $FeCl_3·6H_2O$, $Ce(NO_3)_3·6H_2O$, $NaBH_4$, $NaSO_4$, acetone (C_3H_6O), ethanol (EtOH), formic acid (HCOOH), tert-butyl alcohol (TBA), p-Ben-zoquinone (BQ), salicylic acid (SA), 2, 5-dihydroxybenzoic acid (2, 5-DHBA) and 2, 3-dihydroxybenzoic acid (2, 3-DHBA), tetracycline (TC), metronidazole (MTZ), diclofenac sodium (DFS), chloramphenicol (CAP), ciprofloxacin (CIP) and oxytetracycline hydrochloride (OTC) were of analytical grade and used without further purification. The activated carbon fiber felt was purchased from Nantong Shuangan Activated Carbon Filter Material Co., Ltd. (SA1000-1500, Jiangsu, China). All experimental solutions were obtained using deionized water produced from Milli-Q system.

Preparation of Fe_2O_3: Adding 0.12g of $FeCl_3·6H_2O$ into a 30 mL aqueous solution of ferric chloride. Prepare 20 mL of 5.0 M NaOH aqueous solution, wait for all to dissolve and cool to room temperature before bringing the NaOH solution to volume. Transfer 25mL of ferric chloride solution to a Prex bottle and stir in a 100 ℃ oil bath for five minutes to raise the reaction solution to 100 ℃. Next, add 25mL of NaOH aqueous solution dropwise to the ferric chloride solution at a fixed frequency under intense stirring. After dripping, continue stirring for ten minutes until the solution turns into a cloudy orange red liquid. Stop stirring and quickly transfer the Prex bottle to a 100 ℃ oven, allowing it to age at 100 ℃ for 48 hours. After the reaction, centrifuge at a speed of 3000 rpm for one minute and wash with water and ethanol.

Preparation of Fe_2O_3-CeO_2 NA catalyst： The aforementioned 0.22g of the prepared Fe_2O_3 solid powder was combined with 0.35g $Ce(NO_3)_3·6H_2O$ and 0.5 μg of urea were dissolved in 200 mL ultrapure water, and then 0.4 M of $NaBH_4$ was added dropwise into the above solution. Using a magnetic stirrer to maintain the uniformity of the solution. Transfer the obtained solution to a 100 mL polytetrafluoroethylene lined stainless steel high-pressure vessel. The above mixture reacts at 110 ℃ for 20 hours. Finally, the prepared material was washed with ultra-pure water and ethanol, and then dried in a vacuum oven.

Characterizations: XRD data was acquired from a LabX XRD-6100 X-ray diffractometer with a Cu Kα radiation (40 kV, 30 mA) of wavelength of 0.154 nm

(SHIMADZU, Japan). SEM images were collected on a Gemini SEM 300 scanning electron microscope (ZEISS, Germany) at an accelerating voltage of 5 kV. TEM images were acquired on a HITACHI H-8100 electron microscope (Hitachi, Tokyo, Japan) operated at 200kV. XPS measurements were performed on an Thermo Scientific K-Alpha X-ray photoelectron spectrometer using Al-Kα as the exciting source.

Electrochemical measurements: N_2 reduction experiments were carried out in a two-compartment cell under ambient condition, which was separated by Nafion 117 membrane. The membrane was protonated by first boiling in ultrapure water for 1 hour treating in H_2O_2 (5 wt%) aqueous solution at 80 °C for another 1 h, respectively. And then, the membrane was treaded in 0.5 M H_2SO_4 for 3 h at 80 °C and finally in water for 6 h. The electrochemical experiments were carried out with an electrochemical workstation (CHI 660E) using a three-electrode configuration with prepared electrodes, graphite rod and Ag/AgCl electrode (saturated KCl electrolyte) as working electrode, counter electrode and reference electrode, respectively. The potentials reported in this work were converted to reversible hydrogen electrode (RHE) scale via calibration with the following equation: E (vs. RHE) = E (vs.Ag/AgCl) + 0.059 × pH + 0.197 V and the presented current density was normalized to the geometric surface area. For electrochemical N_2 reduction, chrono-amperometry tests were conducted in N_2-saturated 0.1 M Na_2SO_4 solution.

Determination of NH_3: Specifically, 4 mL electrolyte was obtained from the cathodic chamber and mixed with 50 μL oxidizing solution containing NaClO (ρCl = 4 ~ 4.9) and NaOH (0.75 M), 500 μL coloring solution containing 0.4 M $C_7H_6O_3Na$ and 0.325 M NaOH, and 50 μL catalyst solution (1 wt% $Na_2[Fe(CN)_5NO]$) for 1 h. Absorbance measurements were performed at 654 nm. The concentration-absorbance curve was calibrated using standard NH_3 solution with a series of concentrations. The fitting curve shows good linear relation of absorbance value with NH_3 concentration.

Determination of N_2H_4: A mixed solution of 1.97 g $C_9H_{11}NO$, 10 mL concentrated HCl and 100 ml ethanol was used as a color reagent. Calibration curve was plotted as follow: firstly, preparing a series of N_2H_4 solutions of known concentration as standards; secondly, adding 4 mL color reagent to above N_2H_4 solution, separately, and standing 20 min at

room temperature; finally, the absorbance of the resulting solution was measured at 460 nm. The fitting curve shows good linear relation of absorbance with N_2H_4 concentration.

Determination of FE and NH_3 yield: The FE for N_2 reduction was defined as the amount of electric charge used for synthesizing NH_3 divided the total charge passed through the electrodes during the electrolysis. The total amount of NH_3 produced was measured using colorimetric methods.

Details of NRR Stability Test: Using a H-type electrolytic cell, and with the cathode chamber and the anode chamber strictly isolated by anion exchange membrane to prevent the oxidative species generated by the anode or cross-interference. Samples of a certain volume (1 mL) of electrolyte are taken from the cathode chamber using a syringe every hour for analysis, and the total volume change of the electrolyte is recorded. Quantitative analysis was conducted using the indophenol blue method, and the ammonia production rate and Faraday efficiency for each time period were calculated.

Computational Details: Spin-polarized DFT calculations were performed by using the plane wave-based Vienna ab initio simulation package (VASP).[1,2] The generalized gradient approximation method with Perdew-Burke-Ernzerhof (PBE) functional was used to describe the exchange-correlation interaction among electrons.[3] U (Ce) value of 3.5 eV and U (Fe) value of 2.0 eV were applied to the Ce and Fe states, consistent with the other works. The van der Waals (vdW) correction with the Grimme approach (DFT-D3) was included in the interaction between single molecule/atoms and substrates. The energy cutoff for the plane wave-basis expansion was set to 500 eV and the atomic relaxation was continued until the force sacting on atoms were smaller than 0.01 eV $Å^{-1}$. The CeO_2 (210) surface was modeled using a 2 × 2 slab. The interface models of Fe_2O_3-CeO_2 was constructed by the slab model of 4 × 4 × 1 supercell Fe_2O_3 slab and 5 × 5 × 1 supercell of CeO_2 slab. Periodic boundary conditions were employed along x and y directions with a vacuum region of 15 Å. During the optimization process, the bottom two layers of atoms are fixed and the other layers are relaxed. The cutoff energy for the plane-wave-basis expansion is set to be 500 eV. The Brillouin zone was sampled with 3 × 3 × 1 Gamma-center k-point mesh, and the electronic states were smeared using the Fermi7scheme with

a broadening width of 0.1 eV. The free energies of the reaction intermediates were obtained by $\Delta G = \Delta Eads + \Delta ZPE - T\Delta S + \Delta G(U) + \Delta G(pH)$, where $\Delta Eads$ is the adsorption energy, ZPE is the zero point energy and S is the entropy at 298 K. The effect of a bias was included in calculating the free energy change of elementary reactions involving transfer of electrons by adding $\Delta G(U) = -neU$, where n is number of electrons transferred and Uis the electrode potential.[7] In our calculations, we used U = –0.55 V (vs. RHE). $\Delta G(pH) = -kBTln10 \times pH$, where kB is the Boltzmann constant, and pH = 7 for electrolyte.

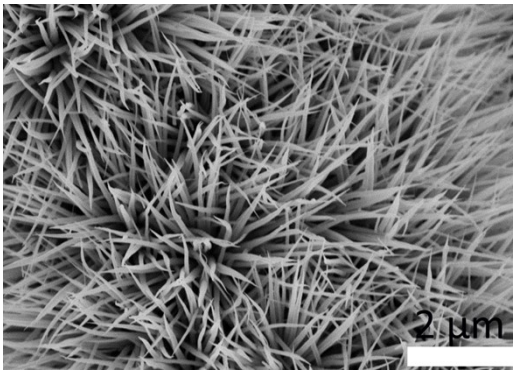

Fig. S1. SEM image of pure CeO_2.

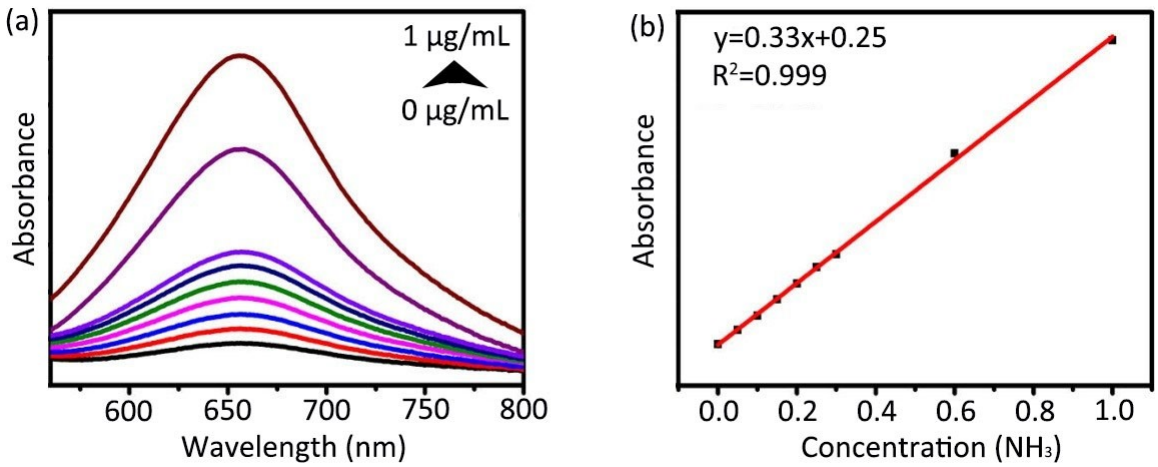

Fig. S2. (a) UV-vis absorption spectra of indophenol assays with NH_3 concentrations after incubated for 1 h at room temperature. (b) Calibration curve used for estimation of NH_3 concentration.

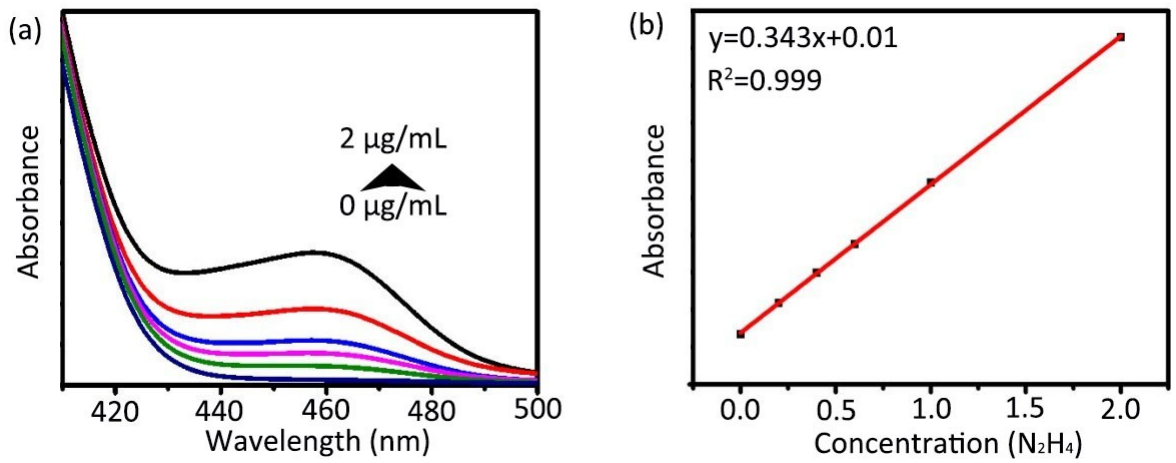

Fig. S3. (a) UV-vis absorption spectra of indophenol assays with N_2H_4 concentrations after incubated for 1 h at room temperature. (b) Calibration curve used for estimation of N_2H_4 concentration.

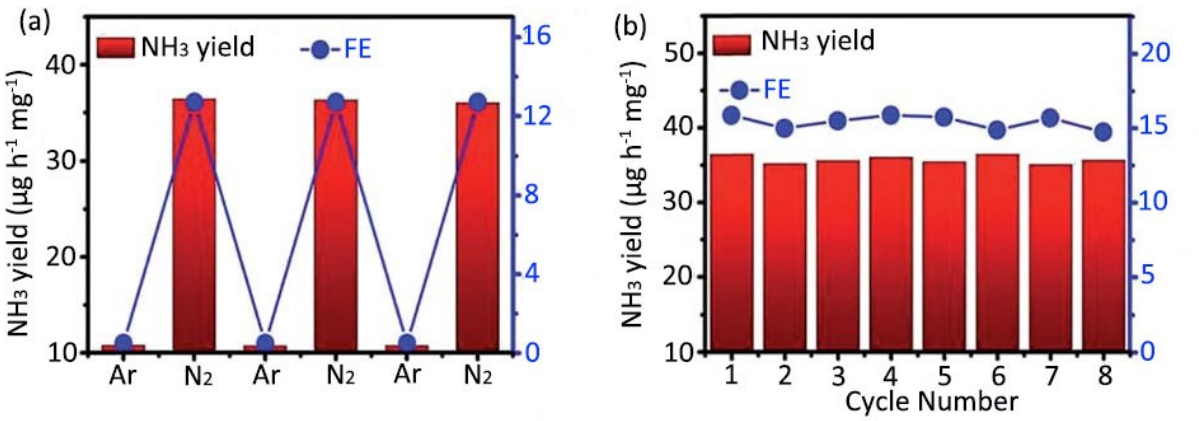

Fig. S4. (c) NH_3 yields and FEs of Fe_2O_3-CeO_2 NA with alternating 3 h cycles between N_2- and Ar-saturated electrolytes. (d) Cycling stability test of Fe_2O_3-CeO_2 NA.

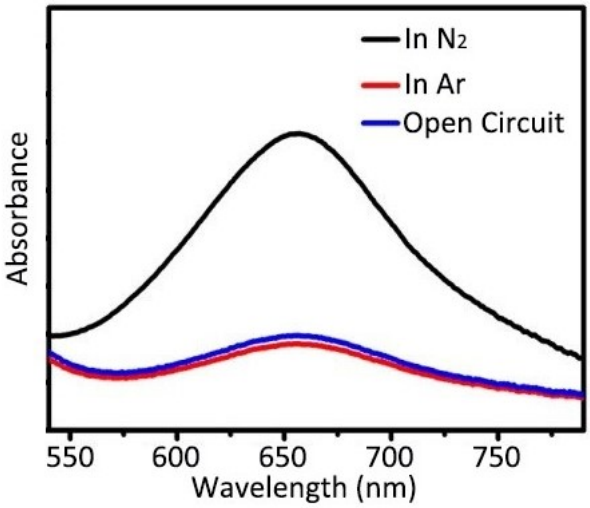

Fig. S5. UV-Vis absorption spectra of the electrolytes at different atmospheres.

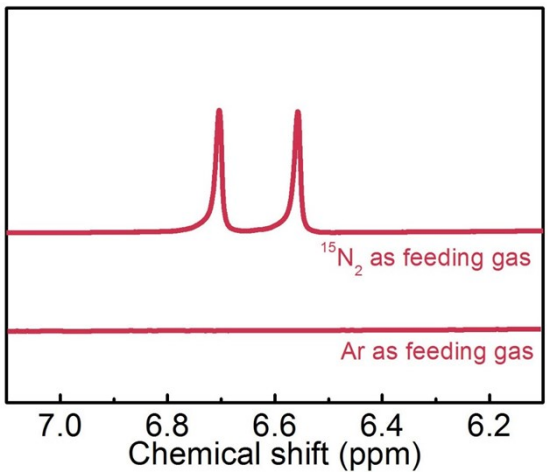

Fig. S6. ^{1}H NMR measurements over Fe_2O_3-CeO_2 NA using $^{15}N_2$ and Ar as feed gases.

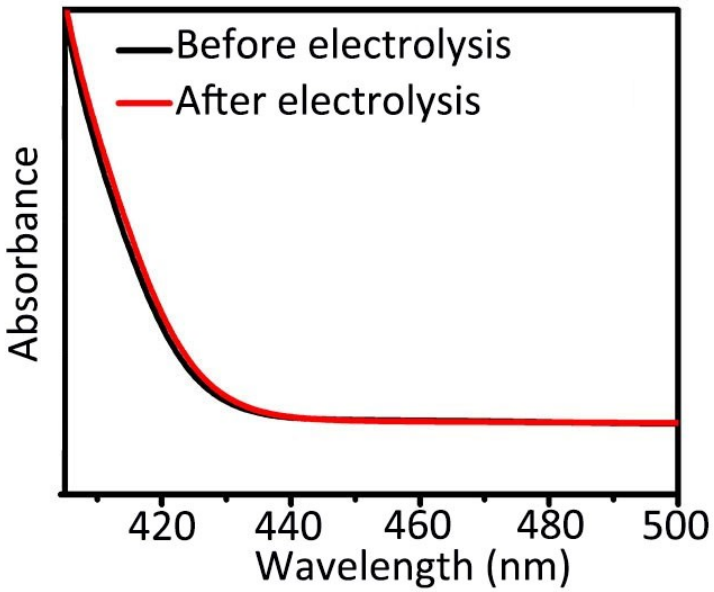

Fig. S7. UV-Vis absorption spectra of electrolytes stained with para-(dimethylamino) benzaldehyde indicator before and after 2 h electrolysis.

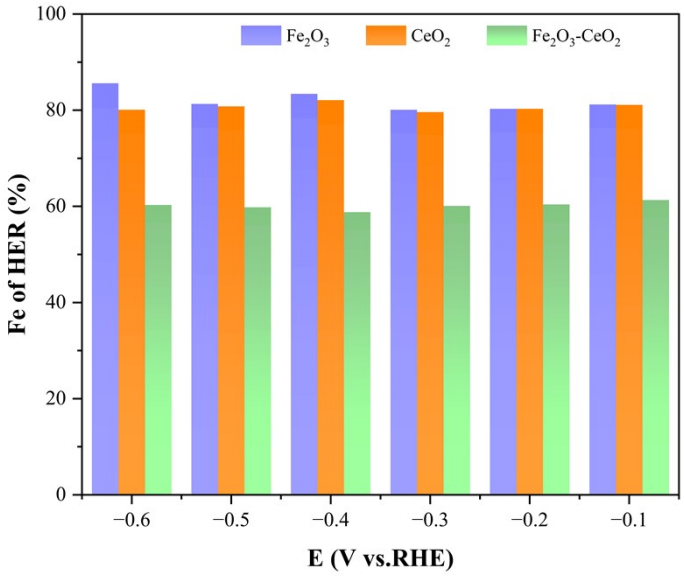

Fig. S8. The FEs of HER at each given potential.

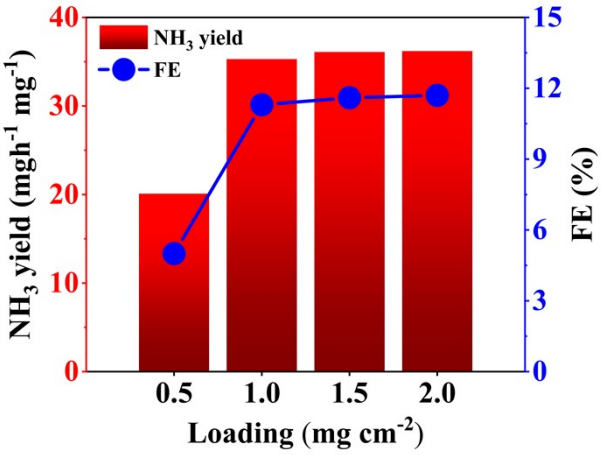

Fig. S9. The NRR performance of Fe_2O_3-CeO_2 NA with different loading.

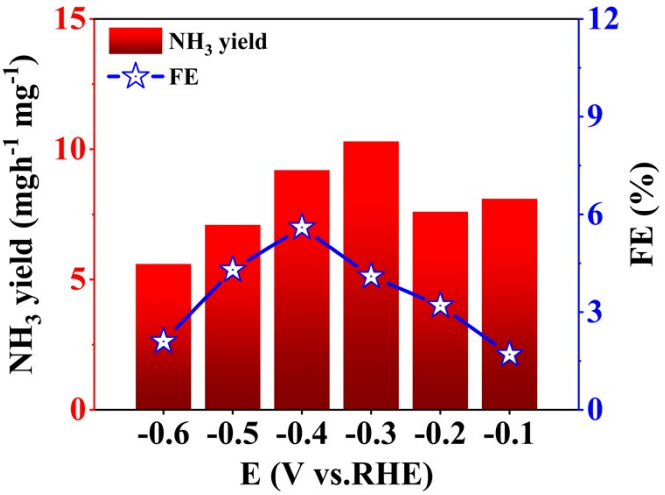

Fig. S10. The NRR performance of Fe_2O_3-CeO_2 NA in 0.1 M HCl.

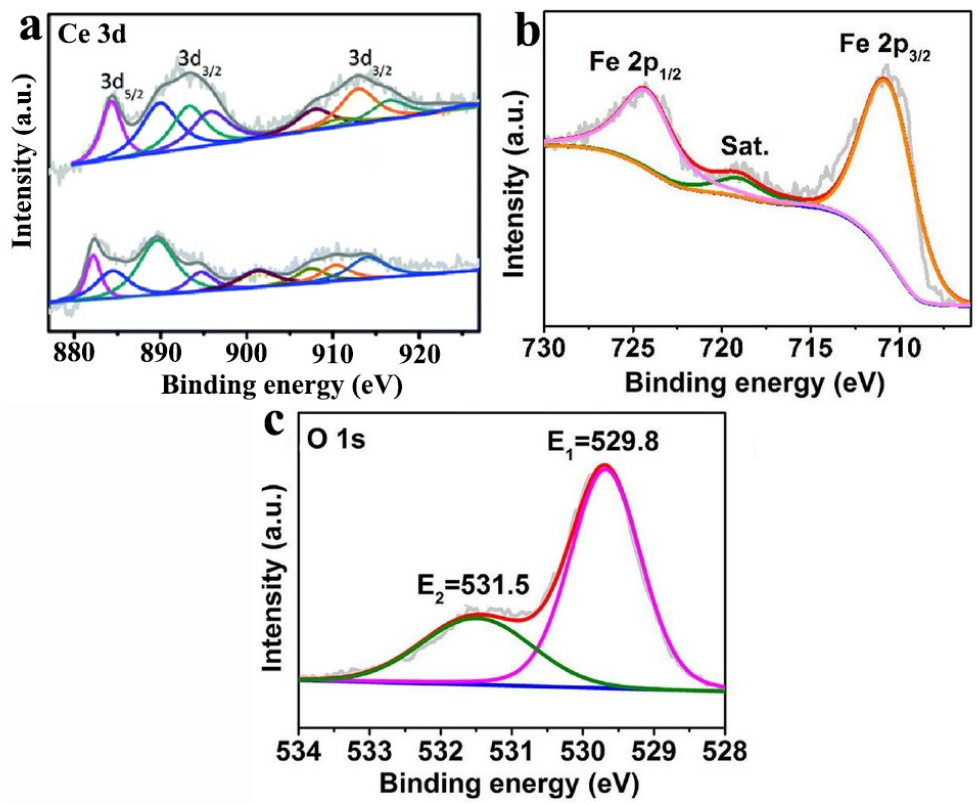

Fig. S11. The NRR performance of Fe_2O_3-CeO_2 NA after long-term test.

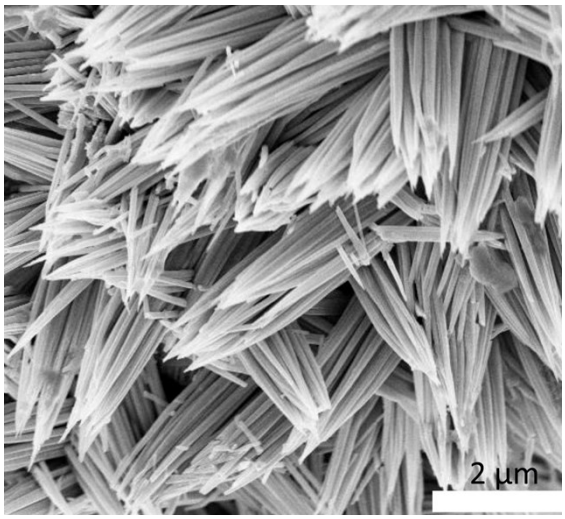

Fig. S12. SEM image of Fe_2O_3-CeO_2 NA after long-term test.

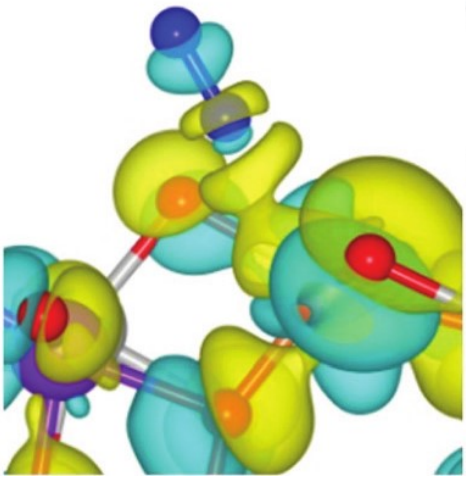

Fig. S13. Electron density difference upon adsorption of an N_2 atom on the Fe_2O_3-CeO_2 NA surface. The topological construction represents electron accumulation (yellow) and depletion (blue), respectively.

Table S1. Comparison of the NRR performance for Fe_2O_3-CeO_2 with recently reported electrocatalysts in alkaline seawater.

Catalyst	Electrolyte	NH_3 yield rate ($\mu g\ h^{-1}\ mg_{cat.}^{-1}$)	FE (%)	Ref.
Fe_2O_3-CeO_2	**0.1 M Na_2SO_4**	**36.76**	**12.6**	**This work**
Fe_2O_3@PPy	-	22.1	24.6	3
D-FeN/C	0.1 M KOH	24.8	15.8	4
$PdFe_3$@G	0.1 M KOH	29.07	22.8	5
$Fe_{3\%}$-$Cu_{2-x}S$	0.1 M Na_2SO_4	26.4	3.1	6
Fe-MoS_2 nanosheet	0.1 M KOH	4.23	10	7
Bi-MoO_x@RGO	0.1 M Na_2SO_4	19.93	17.17	8
Fe_2O_3/Fe_3O_4-CeO_2	0.1 M Na_2SO_4	30.9	26.3	9
Cu−Fe_2O_3	-	12.5	16.4	10
Ru/Fe_2O_3-NC	0.1 M K_2SO_4	141.18	48.89	11
Vs-MoS_2/Vo-Fe_2O_3	0.1 M HCl	73.14 ± 1.35	42.68 ± 2.12	12
α -Fe_2O_3@*m*TiO_2	0.1 M Na_2SO_4	27.2	13.3	13
CeO_2 Nanorod	0.1 M Na_2SO_4	16.4	3.7	14
H-CeO_2	-	25.64	6.3	15

Sn-CeO_{2-x}	-	41.1	35.3	16
CeO_2/ZnO	0.1M Li_2SO_4	60.21	11.48	17
CeO_2/RuO_2	-	50.56	2.96	18
Zn-doped Fe_2O_3	-	15.1	10.4	19

References

1 G. W. Watt, J. D. Chrisp, Spectrophotometric method for determination of hydrazine. *Anal. Chem*., 1952, **24**, 2006–2008.

2 G. Kresse, J. Furthmüller, Efficient iterative schemes for Ab initio total-energy calculations using a plane-wave basis set. *Phys. Rev. B.*, 1996, **54**, 11169.

3 F. Jin, H. Yin, R. Feng, W. Niu, W. Zhang, J. Liu, A. Du, W. Yang, Z. Liu, Charge transfer and vacancy engineering of Fe_2O_3 nanoparticle catalysts forhighly selective N_2 reduction towards NH_3 synthesis. *J. Colloid. Interf. Sci*., 2023, **647**, 354-363.

4 Y. Kong, L. Wu, X. Yang, Y. Li, S. Zheng, B. Yang, Z. Li, Q. Zhang, S. Zhou, L. Lei, G. Wu, Y. Hou, Accelerating protonation kinetics for ammonia electrosynthesis on single iron sites embedded in carbon with intrinsic defects. *Adv. Funct. Mater.*, 2022, **32**, 2205409.

5 J. Mu, Z. Zhao, X. W. Gao, Z. M. Liu, W. B. Luo, Z. Sun, Q. F. Gu, F. Li, Bimetallic $PdFe_3$ nano-alloy with tunable electron configuration for boosting electrochemical nitrogen fixation. *Adv. Energy Mater.*, 2024, **14**, 2303558.

6 D. Zhang, Y. Liu, B. Mao, H. Li, T. Jiang, D. Zhang, W. Dong, W. Shi, Double-phase heterostructure within Fe-doped $Cu_{2-x}S$ quantum dots with boosted electrocatalytic nitrogen reduction. *ACS Sustainable Chem. Eng.*, 2021, **9**, 2844-2853.

7 J. Guo, T. T. Tsega, I. U. Islam, A. Iqbal, J. Zai, X. Qian, Fe doping promoted electrocatalytic N_2 reduction reaction of 2H MoS_2. *Chin. Chem. Lett.*, 2020, **31**, 2487-2490.

8 Y. Wan, Z. Wang, M. Zheng, J. Li, R. Lv, Heterogeneous crystalline–amorphous interface for boosted electrocatalytic nitrogen reduction to ammonia. *J. Mater. Chem. A*, 2023, **11**, 818-827.

9 M. Zhao, J. Wang, X. Wang, J. Xu, L. Liu, W. Yang, J. Feng, S. Song, H. Zhang, Creating highly active iron sites in electrochemical N_2 reduction by fabricating strongly-coupled Interfaces. *Small*， 2023, **19**, 2205313.

10 T. Takashima, H. Fukasawa, T. Mochida, H. Irie, Cu-doped Fe_2O_3 nanorods for enhanced electrocatalytic nitrogen fixation to ammonia. *ACS Appl. Nano Mater.*, 2023, **6**, 23381-23389.

11 Z. Han, N. He, C. Zhu, X. Lan, Y. Xu, Y. kang, Y. Liu, C. Zhou, L. Tong, B. Lu, X. Liu, Q. Wang, M. Yang, S. Han. A high-performance electrocatalyst for sustainable ammonia synthesis via single-atom Ru-embedded Fe_2O_3 nitrogen-DOPED carbon. *Appl. Surf. Sci.*, 2024, **675**, 160975.

12 X. Chen, S. Wu, J. Wang, B. Li, L. Xiao, J. Lv, Q. Liu, Y. Cui, J. Ma, W. Ren, Y. Zhao, Li. Yan, J. Wang, H. Zang, Nitrogenase-inspired Vs-MoS_2/Vo-Fe_2O_3 heterojunction with fixed molar ratio promotes bifunctional nitrogen fixation. *ACS Catal.*, 2025, **15**, 9191-9200.

13 W. Qiu, Y. Luo, R. Liang, J. Qiu, High-performance artificial nitrogen fixation at ambient conditions using a metal-free electrocatalyst. *Nat. Commun.*, 2018, **9**, 3485.

14 B. Xu, L. Xia, F. Zhou, R. Zhao, H. Chen, T. Wang, Q. Zhou, Q. Liu, G. Cui, X. Xiong, F. Gong, X. Sun. Enhancing electrocatalytic N_2 reduction to NH_3 by CeO_2 nanorod with oxygen vacancies. *ACS Sustain Chem Eng.*, 2019, **7,** 2889-2893.

15 J. Li, Y. Wang, X. Lu, K. Guo, C. Xu, Increased oxygen vacancies in CeO_2 for improved electrocatalytic nitrogen reduction performance. *Inorg. Chem.*, 2022, **61**, 17242-17247.

16 Y. Xiao, X. Tian, Y. Guo, J. Chen, W. He, H. Cui, C. Wang, Surface modification of CeO_{2-x} nanorods with Sn doping for enhanced nitrogen electroreduction. *J. Energ. Chem.*, 2023, **87**, 400-407.

17 J. Li, J. Wang, G. Wang, S. Zhao, Z. Yang, X. Wang, Y. Yan， CeO_2/ZnO heterojunction as efficient catalyst for electrocatalytic nitrogen reduction reaction via an “electron pump” effect. *J. Rare Earths*, 2025, **03**, 012.

18 H. Ju, D. Seo, S Chung, X. Mao, B. An, M. Musameh, T. Gengenbach, H. Shon, A. Du, A. Bendavid, K. Ostrikov, H. Yoon, J. Lee, S. Giddey, Green ammonia synthesis using CeO_2/RuO_2 nanolayers on vertical graphene catalyst via electrochemical route in alkaline electrolyte. *Nanoscale*, 2022, **14**,1395-1408.

19 S. Yu, Q. Wang, J. Wang, Y. Xiang, X. Niu, T. Li, Zinc doped Fe_2O_3 for boosting electrocatalytic nitrogen fixation to ammonia under mild conditions. *Int. J. Hydrogen Energy*, 2021, **46**, 14331-14337.

Table S2. NRR performance at different potential.

Fe_2O_3-CeO_2	NH_3 yield (μg h^{-1} $mgcat.^{-1}$)	FE (%)
-0.1 V	20.12	4.8
-0.2 V	23.65	8.0
-0.3 V	36.76	12.6
-0.4 V	29.36	4.2
-0.5 V	23.24	2.1
-0.6 V	20.12	1.8